High-resolution imaging of SNR IC443 and W44 with the Sardinia Radio Telescope

E. Egron[1], **A. Pellizzoni**[1], **M. N. Iacolina**[1], **S. Loru**[1,2],
M. Marongiu[1], **S. Righini**[3], **M. Cardillo**[4], **A. Giuliani**[5],
S. Mulas[2], **G. Murtas**[2] **and D. Simeone**[2]

[1]INAF, Osservatorio Astronomico di Cagliari, Via della Scienza 5, 09047 Selargius, Italy

[2]Dip. di Fisica, Università degli Studi di Cagliari, SP Monserrato-Sestu, KM 0.7, 09042 Monserrato, Italy

[3]INAF, Istituto di Radio Astronomia di Bologna, Via P. Gobetti 101, 40129 Bologna, Italy

[4]INAF, Osservatorio Astrofisico di Arcetri, Largo E. Fermi 5, 50125 Firenze, Italy

[5]INAF, Istituto di Astrofisica Spaziale e Fisica cosmica di Milano, via E. Bassini 15, 20133 Milano, Italy

email: `egron@oa-cagliari.inaf.it`

Abstract. We present single-dish imaging of the well-known Supernova Remnants (SNRs) IC443 and W44 at 1.5 GHz and 7 GHz with the recently commissioned 64-m diameter Sardinia Radio Telescope (SRT). Our images were obtained through on-the-fly mapping techniques, providing antenna beam oversampling, automatic baseline subtraction and radio-frequency interference removal. It results in high-quality maps of the SNRs at 7 GHz, which are usually lacking and not easily achievable through interferometry at this frequency due to the very large SNR structures. SRT continuum maps of our targets are consistent with VLA maps carried out at lower frequencies (at 324 MHz and 1.4 GHz), providing a view of the complex filamentary morphology. New estimates of the total flux density are given within 3% and 5% error at 1.5 GHz and 7 GHz respectively, in addition to flux measurements in different regions of the SNRs.

Keywords. ISM: supernova remnants, ISM: individual (IC443, W44), radio continuum: ISM

1. Introduction

Although radio emission is the most common identifier of Supernova Remnants (SNRs) and a prime probe for refining models, high-resolution images at frequencies above 5 GHz are scarce even for bright and well-known SNRs such as IC443 and W44. These SNRs belong to the remnant "mixed morphology" class (Rho & Petre 1998), characterised by a highly filamentary radio shell (synchrotron emission) and a centrally concentrated X-ray emission. Providing good angular resolution and sensitivity maps at high radio frequencies could help to better constrain the multi-wavelength scenario since local changes in the radio spectrum trace the actual energy distribution of the different electron populations responsible for both radio and part of gamma-ray emissions.

In the frameworks of the Astronomical Validation (AV) and Early Science Program (ESP) with the 64-m single-dish Sardinia Radio Telescope (SRT), we produced, for the first time, single-dish deep imaging at 7 GHz of IC443 and W44 in addition to imaging them at 1.5 GHz. We obtained accurate flux density measurements through on-the-fly (OTF) mapping procedures and using state-of-the-art imaging techniques.

2. Observations with SRT

Located on the Sardinia island in Italy, SRT is designed to observe in the $0.3-115$ GHz frequency range. At present, three receivers are available for observers: a 7-feed K-band receiver ($18-26.5$ GHz), a mono-feed C-band receiver ($5.7-7.7$ GHz), and a coaxial dual-feed L-P band ($1.3-1.8$ GHz; $305-410$ MHz) receiver (Bolli *et al.* 2015).

A first series of observations of IC443 and W44 was performed during the AV of SRT, from May 27 to December 10 2014 ($\sim$12 hrs of effective time on targets). This phase was devoted to testing the performance of the telescope and the acquisition systems (Prandoni *et al.* 2017). The targets were observed at 7.24 GHz with a bandwidth of 680 MHz, using the Total-Power (TP) backend. Subsequently, a program dedicated to the observations of SNRs was approved during the Early Science phase of SRT, for a total exposure time on targets of $\sim$ 20 hrs in C and L-bands. The observations were performed in "shared-risk mode" at 7.0 GHz (bandwidth=1,200 MHz), and 1.55 GHz (bandwidth=460 MHz) between February 14 and March 24 2016, operating simultaneously the TP and SARDARA (SArdinia Roach2-based Digital Architecture for Radio Astronomy; Melis *et al.* in preparation) backends in piggy-back mode.

We carried out the mapping of IC443 and W44 through On-the-Fly (OTF) scans. This technique implies that the data acquisition is continuously ongoing while the antenna performs constant-speed scans across the sky (typically a few degrees/min), alternatively producing maps along the Right Ascension (RA) and Declination (Dec) directions. In particular, the sampling time was set to 40 ms during AV activities and 20 ms during the ESP, which implies the acquisition of $> 10-20$ samples/beam for each scan passage (largely oversampling the beam w.r.t. Nyquist sampling) and an accurate evaluation of flux errors. In addition, beam oversampling allows us to efficiently reject outlier measurements ascribed to radio frequency interference (RFI). The length of the scans is chosen according to the size of the source (typically of the order of $0.5-1°$ for SNRs). In order to properly reconstruct the morphology of the observed source and its associated flux, the scan-dependent baseline (background flux) must be correctly subtracted. Ideally, each scan should be free from significant source contribution (and RFI contamination) for $40-60\%$ of its length/duration, in order to properly identify and subtract the baseline component. This requirement is not trivially satisfied for targets located in crowded regions of the Galactic Plane, as for the case of W44.

Data analysis was performed using the SRT Single-Dish Imager (SDI), which is a tool designed to perform continuum and spectro-polarimetric imaging, optimized for OTF scan mapping, and suitable for all SRT receivers/backends (Egron *et al.* 2016). The core of our prodecure is to fully exploit the availability of a significant number of measurements per beam (and then per pixel, typically chosen to be about 1/4 of the HPBW), in order to have a straightforward evaluation of statistical errors (through standard deviation of the measurements in each pixel), efficient RFI outliers removal and accurate background baseline subtraction.

3. IC443

We produced the maps of IC443 and measured the integrated flux density of the source by defining a centroid of the diffuse emission and considering a radius of $0.5°$ (centroid coord: $06^h 16^m 58.00^s + 22°31'36.0''$). Integrated flux densities of the maps obtained by simultaneous observations using the TP and SARDARA (operating in piggy-back mode) during the ESP are fully consistent at 7 GHz and also compatible with AV observations performed more than one year earlier within 1σ. Averaging these results, we obtain a
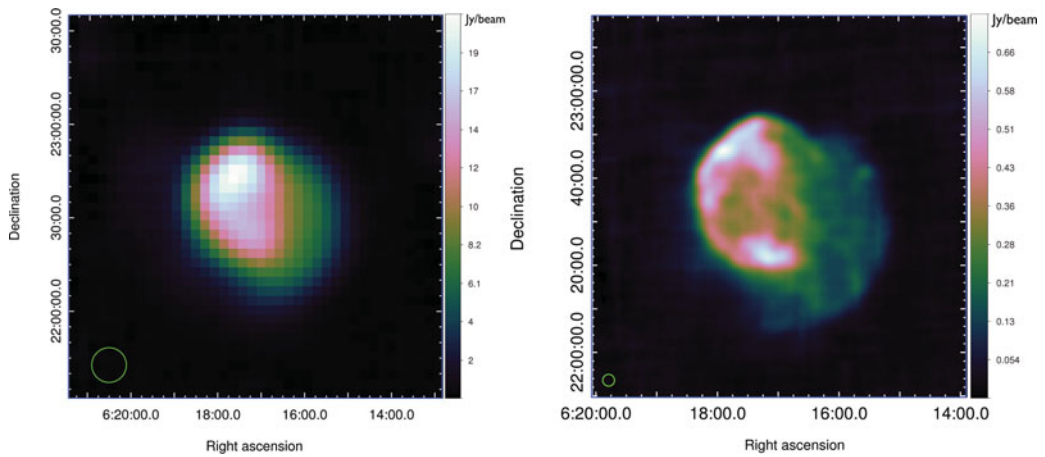
Figure 1. SRT continuum map of SNR IC443 obtained at 1.55 GHz with the SARDARA backend (left) and at 7.2 GHz with the TP backend (right). The green circles on the bottom left indicate the beam size at the observed frequencies. Pixel sizes are 3.0′ and 0.6′ for 1.55 GHz and 7.2 GHz maps, respectively, which corresponds to 1/4 HPBW.
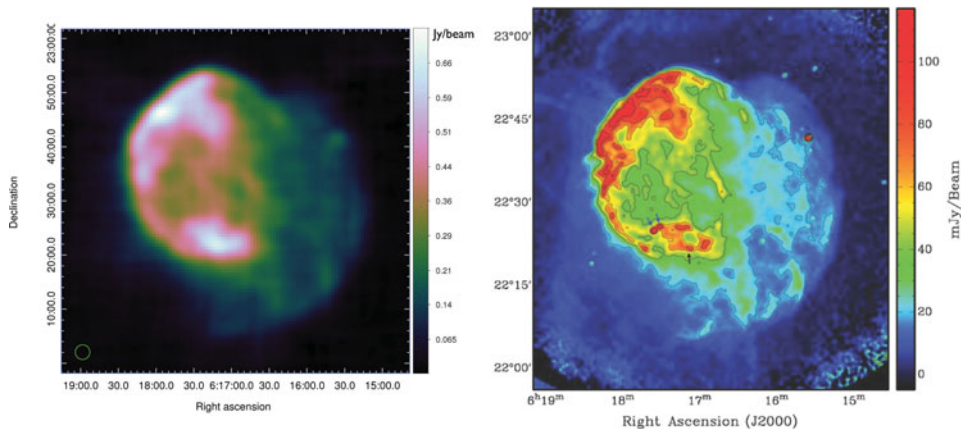

Figure 2. Comparison of the continuum maps of IC443 obtained with SRT at 7 GHz (left) with that obtained combining VLA and Arecibo at 1.4 GHz (right; Lee *et al.* 2008).

continuum flux of 66.8 ± 2.9 Jy at 7 GHz. The integrated flux measured with SARDARA at 1.55 GHz is 133.7 ± 4.0 Jy. The total averaged maps of IC443 obtained at both frequencies are presented in Figure 1.

Our measurements are consistent with continuum flux density measurements reported in the literature at 1.4 GHz ($S_{1.4\,\mathrm{GHz}} = 130 \pm 13$ Jy originally obtained by Green 1986 then scaled accordingly to Baars *et al.* 1977 flux density scales) and at 6.6 GHz ($S_{6.6\,\mathrm{GHz}} = 70 \pm 15$ Jy by Dickel 1971), within 1σ. It is worth noting that typical continuum flux errors for IC443 in the literature are of the order of $\sim 10 - 15\%$, while we provided more accurate measurements. This is mostly due to our oversampled maps in which, for each pixel, tens of OTF baseline-subtracted scans are available, providing straightforward error measurements through standard deviation estimates.

We then compared the SRT map with high-resolution maps of IC443 obtained by combining interferometric and large-area single-dish observations. VLA and Arecibo lower frequency data at 1.4 GHz were combined together to achieve an extremely good
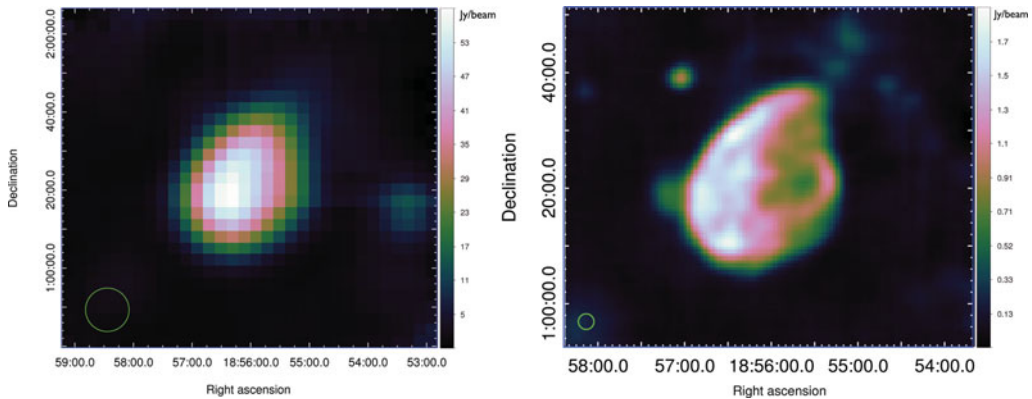
Figure 3. SRT continuum map of SNR W44 obtained at 1.55 GHz with the SARDARA backend (left) and at 7.2 GHz with the TP backend (right). Pixel sizes are as in Fig. 1.

sensitivity and angular resolution of about $40''$ (Lee *et al.* 2008). The main features of the morphology of IC443 revealed with SRT at 7 GHz are consistent with those in the above observations, as testified by Figure 2, and with the image obtained at 330 MHz (not shown in this paper) with the VLA (Castelletti *et al.* 2011).

IC443 consists in two nearly concentric shells, which present a complex structure with the presence of filaments (not resolved, but detected in the SRT image), and a clear difference in the radio continuum intensity. The mean surface brightness associated with the brightest rims of IC443 is ~ 0.6 Jy/beam at 7 GHz (measured with SRT), which is about five times larger than that corresponding to the western halo.

4. W44

The OTF maps of W44 obtained with SRT at 1.55 and 7 GHz are presented in Figure 3. The integrated flux density of W44 was measured by considering a radius of $0.32°$ around $18^h 56^m 05.00^s + 01°21'36.0''$. We obtained 214.4 ± 6.4 Jy at 1.55 GHz and 93.7 ± 4.0 Jy at 7 GHz. The flux obtained at 7.0 GHz with SRT is in agreement with Hollinger & Hobbs (1966): $S_{8.3\,\mathrm{GHz}} = 95 \pm 23$ Jy. The continuum fluxes presented in the literature at ~ 1.4 GHz provide a wide scatter, as shown in Table 1. In particular, measurements at 1.4 GHz by Giacani *et al.* (1997) ($S_{1.4\,\mathrm{GHz}} = 210 \pm 20$ Jy) and Castelletti *et al.* (2007) ($S_{1.4\,\mathrm{GHz}} = 300 \pm 7$ Jy) are inconsistent. The value we measured with SRT at 1.55 GHz is comparable within 1σ with most other L-band flux measurements obtained in the '60s and with Giacani *et al.* (1997). Note also the small error bars on our value.

We then compared our maps with high-resolution VLA images of the remnant at 1,465 MHz (Jones *et al.* 1993) and 324 MHz (Castelletti *et al.* 2007), which were obtained using interferometric multiple-configurations (see Figure 4 for a comparison with the 324 MHz map). The radio emission of W44 is characterized by an asymmetric limb-brightened shell. The brightest filaments are also detected with SRT (although not resolved), and they most likely result from radiative shocks driven into clouds or sheets of dense gas (Jones *et al.* 1993). The brightest emission occurs along the eastern boundary at $\sim 18^h 56^m 50.00^s + 01°17'00.0''$. It results from the interaction between W44 and dense molecular clouds observed in this region (Seta *et al.* 2004). Using Spitzer observations at 24 μm and 8 μm, Castelletti *et al.* (2007) identified a circular HII region centered at $18^h 56^m 47.9^s + 01°17'54.0''$ and named G034.7-00.6 with the IRAS point source 18544+0112, which is a young stellar object located on its border. This feature
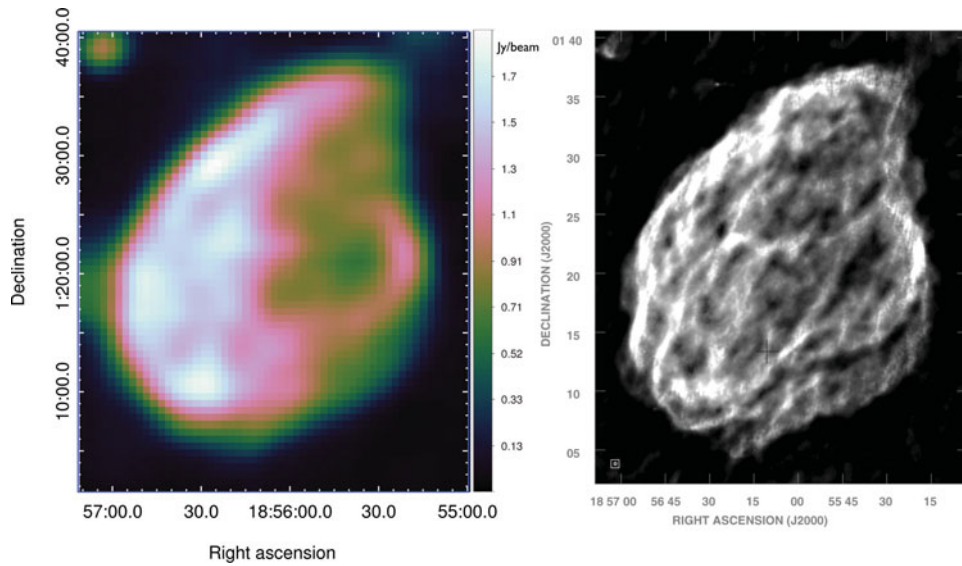
Figure 4. Comparison of the continuum maps of SNR W44 obtained with SRT at 7.0 GHz (left) with that obtained with the VLA at 324 MHz (right) by Castelletti *et al.* (2007). The beam size in the SRT map is represented by the point-like source (known as a HII region G035.040-00.510) in the top left corner.

Table 1. Comparison of the integrated flux densities of W44 measured in the 1.39 to 1.55 GHz frequency range, including the new SRT value at 1.55 GHz. Tabulated values have been reported from the literature as they were originally published.

Frequency (GHz)	Flux density (Jy)	References
1.39	173 ± 35	Westerhout (1958)
1.40	188 ± 23	Pauliny-Toth *et al.* (1966)
1.40	173 ± 26	Kellermann *et al.* (1969)
1.41	236 ± 47	Scheuer (1963)
1.41	236 ± 35	Beard & Kerr (1969)
1.41	275 ± 27	Altenhoff *et al.* (1970)
1.42	180 ± 36	Leslie (1960)
1.44	210 ± 20	Giacani *et al.* (1997)
1.44	300 ± 7	Castelletti *et al.* (2007)
1.55	214 ± 6	Our work

appears at about 0.7 Jy/beam in the SRT 7 GHz image at $18^h 57^m 10.00^s + 01°18'00.0''$. To the west, a short bright arc is visible at $18^h 55^m 20.00^s + 01°22'00.0''$. It corresponds to the SNR shock colliding with a molecular cloud located in this region, which is consistent with bright optical filaments (Giacani *et al.* 1997) and IR observations. The map of W44 includes a classified HII region G035.040-00.510, as listed for example in the WISE Catalog of Galactic HII regions, at $18^h 57^m 04.00^s + 01°38'45.0''$, which is visible in the SRT and VLA images at low frequencies and other wavelengths (IR with Spitzer). The corresponding flux density measured with SRT is 0.94 ± 0.05 Jy at 7.2 GHz.

5. Summary

We obtained accurate images of IC443 and W44 probing the capabilities of the Sardinia Radio Telescope by operating single-dish OTF maps. Our results show reliable performances of the instrumentation over a two-year-long time span (gain stability <5%) and

provide self-consistency checks in measurements performed by simultaneous piggy-back observations with two different backends. We compared the values of the integrated flux densities obtained with SRT at 1.55 GHz and 7 GHz with those presented in the literature. SRT flux estimates are given with a very precise error of 3% and 5% at 1.5 GHz and 7 GHz, respectively

Interferometry can "pass the baton" to single-dish techniques to image large structures ($\sim 1°$ or more) at high frequencies, since synthesis imaging becomes difficult in this context. In fact, the most prominent features highlighted in the SRT maps at 7 GHz are coherent with the high-resolution, low-frequency interferometric images of IC443 and W44. Thus, good mapping quality of large structures can be maintained even at high-frequencies if deep and oversampled OTF single-dish mapping is provided.

This work represents a first scientific milestone for SRT, testifying its capabilities and performances in single-dish imaging, and exploiting different receivers and backends.

6. Work in progress

By coupling the SRT maps at 1.5 and 7 GHz, we obtain spatially-resolved spectral-indices maps of IC443 and W44 (see Pellizzoni *et al.*, these proceedings). Accurate spectral imaging at such high-radio frequencies are necessary in order to understand the physical properties and better constrain the multi-wavelength scenario (leptonic versus hadronic models). Moreover, observations of both targets performed at 21.4 GHz with SRT K-band 7-feed receiver allow us to investigate the complex morphology of these SNRs at high frequency (see Loru *et al.*, these proceedings). We will then perform spectral imaging by coupling 7 and 21 GHz maps.

A new multi-feed S-band receiver $(3 - 4.5$ GHz) is under construction at SRT. At the moment, we performed OTF maps of IC443 and W44 using the central feed as a first test. The high quality of the maps is very promising. SRT represents a great instrument to investigate the morphology and spectrum of SNRs at 1.5, 4, 7 and 21 GHz and search for possible spectral break.

The next steps are the analysis of spectral lines thanks to the SARDARA backend, the production of polarization maps, and performing maps in Q-band $(33 - 50$ GHz) as soon as the receiver will be installed at SRT.

References

Baars, J. W. M., Genzel, R., Pauliny-Toth, I. I. K. *et al.* 1977, *A& A*, 61,99

Bolli, P., Orlati, A., Stringhetti. L, *et al.* 2015, *Journal of Astronomical Instrumentation*, 4, 1550008

Castelletti, G., Dubner, G., Brogan, C., & Kassim, N. E. 2007, *A& A*, 471, 537

Castelletti, G., Dubner, G., Clarke, T., & Kassim, N. E. 2011, *A& A*, 534, A21

Dickel, J. R. 1971, *PASP*, 83,343

Egron, E., Pellizzoni, A., & Iacolina, M. N. 2016, *INAF - Osservatorio Astronomico di Cagliari. Internal Report*, N.59

Green, D. A. 2014, *Bull. Astr. Soc. of India*, 42, 47

Hollinger, J. P. & Hobbs, R. W. 1966, *Science*, 153, 1633

Jones, L. R., Smith, A., & Angelini, L. 1993, *MNRAS*, 265, 631

Lee, J. J., Koo, B. C., Yun, M. S., *et al.* 2008, *ApJ*, 135, 796

Prandoni, I., Murgia, M., Tarchi, A., *et al.* 2017, *A& A* Accepted for publication

Rho, J. & Petre, R. 1998, *ApJL*, 503, L167

Seta, M., Hasegawa, T., & Sakamoto, S. 2004, *ApJ*, 127, 1098